

Analysis of the Linear and Nonlinear Time Response of a P-i-N Photodiode by a Two-Valley Model

P. S. Matavulj, D. M. Gvozdić and J. B. Radunović

Abstract—The linear and nonlinear time response of a P-i-N photodiode are analyzed, in this paper, using the complete phenomenological model for two-valley semiconductors. The analysis has been made for several energies of incident pulse excitation, including the variations of photodiode thickness. The influence of nonlinear and nonstationary effects is shown. For smaller thicknesses of absorption layer nonstationary effects are negligible and nonlinear effects are prominent for larger incident pulse excitation, but for larger thicknesses of absorption layer presence of nonstationary effects amplifies nonlinearity and slow down the time response already at low incident pulse excitation.

I. INTRODUCTION

We analyze the time response (current or voltage) of high speed P-i-N photodetectors made of a two-valley semiconductor (GaAs). We use a complete phenomenological model for two-valley semiconductors presented in [1]. The linear frequency response is considered, only, in this paper. The linear response is studied in [2], [3], too, but many important effects have been negligible and used models have not given opportunities for consideration of the nonlinear response. Analyses in [4], [5], [6], [7], [8] have enabled consideration of the nonlinear response. However, presented models have analyzed the nonlinear response taking only some effects and its influence on transit times, response time and distortion of the time response into consideration. In our paper we have analyzed both the linear and nonlinear time responses and the influence of all relevant effects: diffusion, electron intervalley transfer (nonstationary effects), accumulated photogenerated charge in depletion layer and change of the bias voltage (nonlinear effects), including displacement current and influence of the RC constant. Results are characterized in time domain via shape of the time response, electrons and holes transit times and response time.

II. THE TWO-VALLEY MODEL

The complete phenomenological two-valley model consists of 19 equations.

P. S. Matavulj, D. M. Gvozdić and J. B. Radunović are with the Faculty of Electrical Engineering, University of Belgrade, Bulevar revolucije 73, 11120 Belgrade, Yugoslavia, E-mail: matavulj@kiklop.ETF.bg.ac.yu

The P-i-N photodiode is joined in the electric circuit with load resistance R and polarized at reverse bias voltage V_{CC} . $U(t)$ is the voltage of the reverse biased P-i-N photodiode and $I(t)$ is its photocurrent. In the equivalent circuit of the photodiode resistance of the diode contacts is neglected, as also is the parasitic capacitance of the external circuit, while the P-i-N photodiode capacitance is taken into account via the displacement current. During detection the photodiode voltage is

$$U(t) = V_{CC} - RI(t) . \quad (1)$$

Electric field consists of two parts, one being built in electric field $E_W(x, t)$ in the case of weak optical generation and the other which is the field $E_{SC}(x, t)$ induced by accumulated photogenerated charge in depletion layer. The first component of the electric field is determined by the concentration of fixed charges and the variable reverse-bias voltage (enable consideration one kind of the nonlinearity), and the second component is determined by the concentration of photogenerated carriers (enable consideration other kind of the nonlinearity). The electric field in the i-region (depletion layer) is

$$E(x, t) = E_W(x, t) + E_{SC}(x, t), \quad (2)$$

$$E_W(x, t) = \begin{cases} -\frac{eN}{\epsilon}(w(t) - x), & 0 \leq x \leq w(t) \quad (w(t) \leq d) \\ -\frac{eN}{\epsilon}(d - x) - \frac{U(t) - V_D(d)}{d}, & 0 \leq x \leq d \quad (w(t) > d) \end{cases} \quad (3)$$

$$0, \begin{cases} -L \leq x < 0 \quad \text{and} \quad d < x \leq L \\ \text{or} \\ w(t) \leq x \leq d \quad (w(t) \leq d) \end{cases}$$

$$\frac{dE_{SC}(x, t)}{dx} = \frac{e}{\epsilon}(p(x, t) - n_1(x, t) - n_2(x, t)), \quad (4)$$

where d is the width of the i-region, L and L are widths of p- and n- regions, respectively. $V_D(d) = \frac{eNd^2}{2\epsilon}$ is the

punchthrough voltage (N is the small residual donor concentration in the absorption layer; P^+ and N^+ are acceptor and donor concentration in p- and n- region, respectively), and $w(t) = \sqrt{\frac{2\varepsilon U(t)}{eN}}$ is the width of depletion layer. $\varepsilon = \varepsilon_0\varepsilon_r$ is the dielectric constant of GaAs and e is the electron charge. The subscripts 1 and 2 correspond to electrons in the conduction-band valley 1 (the central valley) and the conduction-band valley 2 (the satellite valleys).

To analyze the detection process in the two-valley semiconductor we have to use the transition rates for intervalley electron transfer in the continuity equations for the central and the satellite valleys electrons. The continuity equations for electrons and holes read

$$\frac{\partial n_1(x, t)}{\partial t} - \frac{1}{e} \frac{\partial}{\partial x} j_1(x, t) = G_{op}(x, t) + g(x, t), \quad (5)$$

$$\frac{\partial n_2(x, t)}{\partial t} - \frac{1}{e} \frac{\partial}{\partial x} j_2(x, t) = -g(x, t), \quad (6)$$

$$\frac{\partial p(x, t)}{\partial t} + \frac{1}{e} \frac{\partial}{\partial x} j_p(x, t) = G_{op}(x, t), \quad (7)$$

and should be solved together with the drift-diffusion equations for the optically generated electrons

$$j_i(x, t) = en_i(x, t)v_i(x, t) + e \frac{\partial}{\partial x} (D_i n_i(x, t)), \quad (8)$$

$$i = 1, 2, \quad (9)$$

$$j_n(x, t) = j_1(x, t) + j_2(x, t), \quad (9)$$

and with the corresponding the drift-diffusion equations for optically generated holes

$$j_p(x, t) = ep(x, t)v_p(x, t) - e \frac{\partial}{\partial x} (D_p p(x, t)), \quad (10)$$

so that the total conduction current density equals

$$j(x, t) = j_n(x, t) + j_p(x, t). \quad (11)$$

D_1 , D_2 and D_p are diffusion constants for electrons in the central and the satellite valleys and for holes, respectively.

The net transfer rate (enable consideration nonstationary effects) is given by

$$g(x, t) = \frac{n_2(x, t)}{\tau_{21}(E(x, t))} - \frac{n_1(x, t)}{\tau_{12}(E(x, t))}, \quad (12)$$

where $\tau_{12}(E(x, t))$ and $\tau_{21}(E(x, t))$ are the phenomenological values of electron transfer times from valley 1 to valley 2 and *vice versa* [4], defined by

$$\tau_{12}(E(x, t)) = 5.64 \left(\frac{2.5}{E(x, t) - 2.5} \right)^{1.3} \quad (13)$$

$$\tau_{21}(E(x, t)) = \text{const.} = 5.64 \text{ ps}$$

In the above equations we neglect recombination, because we assume that the processes considered are fast. We also neglect thermal generation, because it creates the dark current that is negligible when compared with the photocurrent throughout the range of investigation.

The pulsed optical generation rate is

$$G_{op}(x, t) = \alpha I_0(t) e^{-\alpha x}, \quad (14)$$

where $I_0(t)$ is the incident photon flux density

$$I_0(t) = \frac{W}{hc} \delta(t) = I_0 \delta(t), \quad \frac{S}{\lambda}$$

with W being the energy of incident light, λ the wavelength of incident light, S the P-i-N photodiode active area, h Planck's constant and c the velocity of light, and α is the optical absorption coefficient in GaAs.

The velocity versus electric field dependences are [1]

$$v_i(x, t) = \begin{cases} \mu_i E(x, t), & v_i(x, t) \leq v_{is} \\ v_{is}, & \text{otherwise} \end{cases}, \quad i = 1, 2, \quad (15)$$

where are v_{1s} and μ_1 the saturation velocity and mobility of electrons in the central valley, respectively, and v_{2s} and μ_2 the corresponding quantities in the satellite valleys, respectively. Similarly, for holes we have

$$v_p(x, t) = \begin{cases} \mu_p E(x, t), & v_p(x, t) \leq v_{ps} \\ v_{ps}, & \text{otherwise} \end{cases}, \quad (16)$$

where v_{ps} and μ_p are the saturation velocity and mobility of holes, respectively.

The P-i-N photodiode response is given by the relation [4]

$$I(t) = \frac{S}{d} \int_0^d j(x, t) dx + \frac{\varepsilon S}{d} \frac{dU(t)}{dt}. \quad (17)$$

The first term in the above equation is the conduction current, and the second term is the displacement current.

Equations (1)-(17) together with the initial conditions

$$\begin{aligned} n_1(x, 0) = p(x, 0) &= \alpha I_0 e^{-\alpha x} \\ n_2(x, 0) &= 0 \\ E(x, 0) &= E_W(x, 0) \\ U(0) &= V_{CC} \end{aligned} \quad (18)$$

and boundary conditions [4]

$$\begin{aligned} n_1(-L, t) = n_1(L, t) &= 0 \\ n_2(-L, t) = n_2(L, t) &= 0 \\ p(-L, t) = p(L, t) &= 0 \end{aligned} \quad (19)$$

are a closed system that enables one to determine the current or voltage response.

III. NUMERICAL CALCULATION

The closed system of equations was solved by a method of finite differences, observing stability conditions $v_{max}\Delta t \leq \Delta x$ ($v_{max} = v_{1s}$ - maximal carriers velocity) and adopting corresponding temporal step $\Delta t = 10^{-4}ps$ of the numerical simulation.

IV. RESULTS AND DISCUSSION

As a result of the numerical simulation, the current and voltage responses, electrons, in both the central and the satellite valleys, and holes concentrations, and the profiles of electric fields, during detection process, are obtained. We shall first analyze the linear time response.

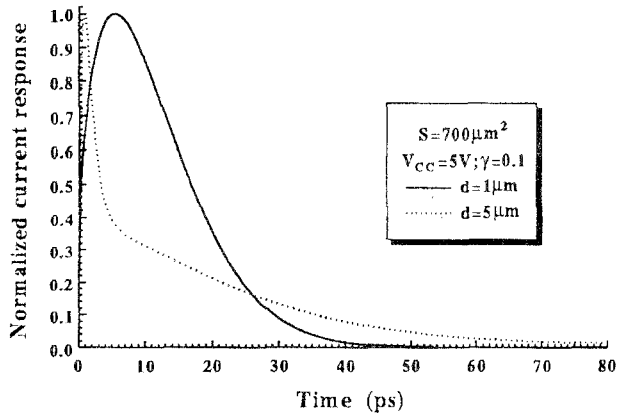


Fig. 1. The linear normalized current responses of the P-i-N photodiode for the active area $S = 700\mu m^2$, bias voltage $V_{CC} = 5V$ (excitation level $\gamma = 0.1$) and two different thicknesses of absorption layer $d = 1\mu m$ and $d = 5\mu m$.

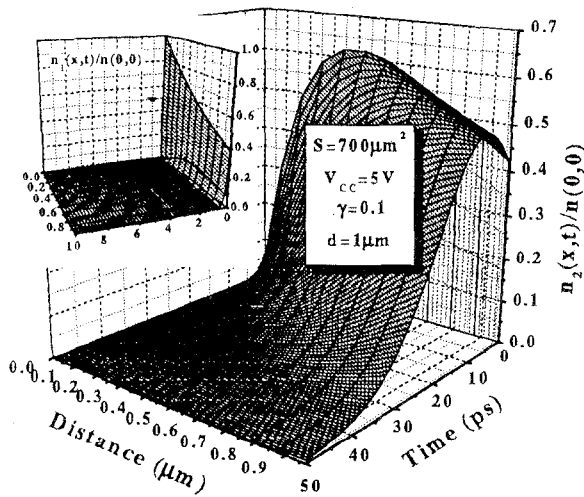


Fig. 2. The profiles of the normalized electron concentration in the central and the satellite valleys for the active area $S = 700\mu m^2$, bias voltage $V_{CC} = 5V$ (excitation level $\gamma = 0.1$) and thickness of absorption layer $d = 1\mu m$.

The linear responses are given in fig. 1. Different curves of the linear response, for two absorption layer

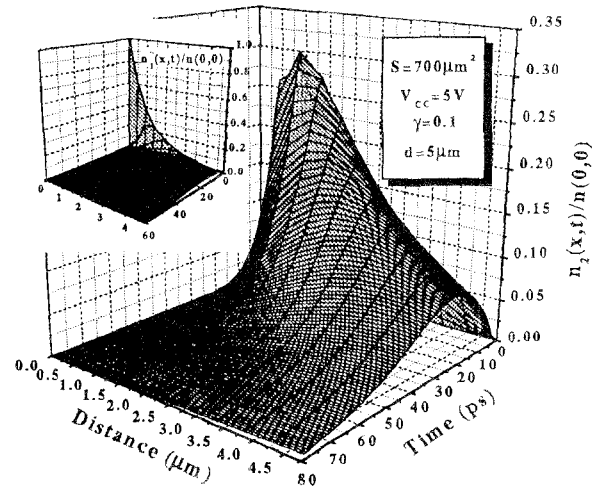


Fig. 3. Same as in Fig. 2 but for thickness of absorption layer $d = 5\mu m$.

thicknesses $d = 1\mu m$ and $d = 5\mu m$ are clearly apparent. Reason for this are smaller electrons transit time and response time for solid curve of the linear response because the electric field is larger (i.e. electrons velocity is larger) and the traveling rout is smaller. For this curve nonstationary effects are not dominant because the electric field is high enough and almost all electrons are traveling through the satellite valleys (electrons intervalley transfer is negligible). It is main reason that this curve isn't deformed. This is obvious from fig. 2 which depicts electron concentration in the central and the satellite valleys in case considered. All electrons are scattered in satellite valleys immediately after illumination of the P-i-N photodiode (after 1ps). The opposite case is for larger absorption layer thickness $d = 5\mu m$. In this case, electrons exist in both the central and the satellite valleys (see fig. 3), and electrons intervalley transfer isn't negligible. Nonstationary effects are more prominent, now, and that's why the time current response is deformed. The time response after 40ps increases response time and decreases bandwidth of the P-i-N photodiode. Although, a smaller portion of electrons is in the satellite valleys than for $d = 1\mu m$, response is slow down because electrons longer retain there (exists in the satellite valleys after 50ps).

A nonlinear case is much complicated. Than, nonlinear effects (especially change of the bias voltage) play main role and significantly increase response time of the P-i-N photodiode. This is obviously from figs. 4 and 5. For $d = 1\mu m$, the extension of time response is consequence of the smaller electric field, because the photodiode voltage significantly drops and slow down photogenerated carriers. The voltage drop is consequence of the strong current in beginning, caused by a strong optical excitation. For $d = 5\mu m$, nonlinear effects are dominant at lower excitation levels because the electric

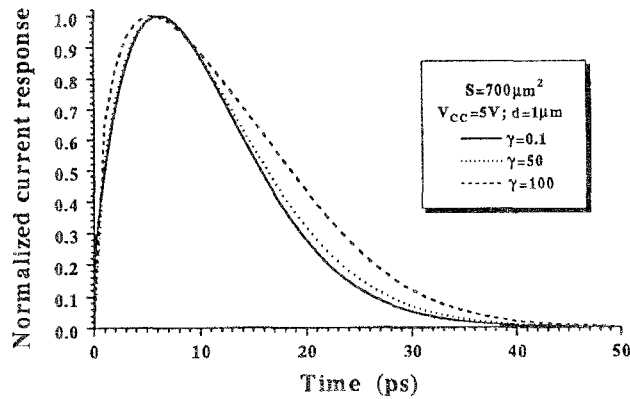


Fig. 4. The comparison of the linear and nonlinear normalized current responses of the P-i-N photodiode with absorption layer thickness $d = 1 \mu\text{m}$. A linear case is for excitation level $\gamma = 0.1$, and a nonlinear case is for excitation levels $\gamma \geq 10$.

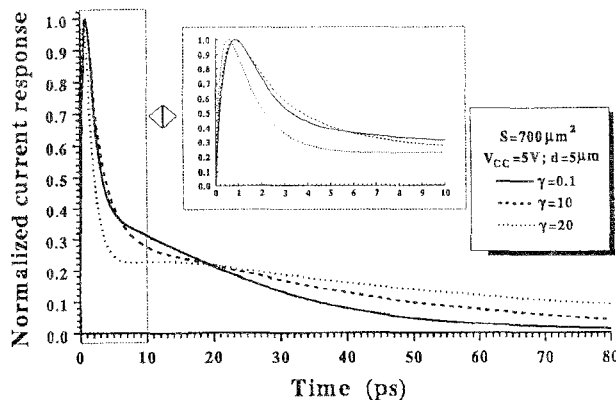


Fig. 5. Same as Fig. 4, but for absorption layer thickness $d = 5 \mu\text{m}$.

field is smaller. Influence of nonstationary and nonlinear effects is shown in fig. 6 via normalized electron concentration in both the central and the satellite valleys and perturbation of the electric field. In this case, the described nonlinear effects are combined with nonstationary effects and a larger deformation of the time response is apparent. This cause additional increase of response time.

V. CONCLUSION

Using presented investigation we have derived following conclusions. For smaller thicknesses of the absorption layer nonstationary effects could be negligible. In that case the time response is only the nonlinear response for enough high incident optical excitation. However, for larger thicknesses of the absorption layer nonstationary effects are dominant, and the time response is the nonlinear nonsaturation response if incident optical excitation is $\gamma \geq 10$. It means that the influence of nonlinear effects on the time response is more prominent for larger than for smaller thicknesses of the absorption layer at the same incident optical excitation. The presence of nonstationary effects has de-

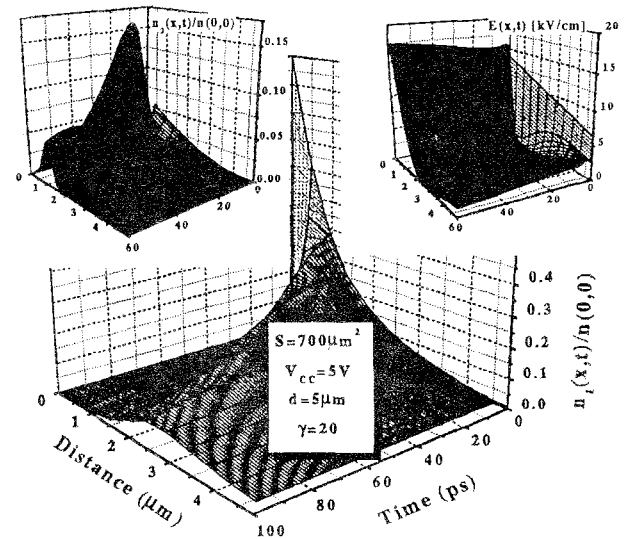


Fig. 6. The profiles of the electric fields and the normalized electron concentration in the central and the satellite valleys for the active area $S = 700 \mu\text{m}^2$, bias voltage $V_{CC} = 5V$ (excitation level $\gamma = 20$) and thickness of absorption layer $d = 5 \mu\text{m}$.

formed shape of the time response. That's why one may note that the characterization of the current response with FWHM (Full Width at Half Maximum) is possible only when nonstationary effects are not dominant, in both cases the linear and nonlinear responses. This characterization may not be use in the linear (and nonlinear) case when electrons intervalley transfer is prominent.

REFERENCES

- [1] P. S. Matavulj, D. M. Gvozdić, and J. B. Radunović, "The Influence of Nonstationary Carrier Transport on the Bandwidth of P-i-N Photodiode," *Publications of the Faculty of Electrical Engineering, University of Belgrade, Series:Engineering Physics*, pp. 3-18, 1996.
- [2] J. E. Bowers and C. A. Burrus, "Ultrawide-Band Long-Wavelength p-i-n Photodetectors," *Journal of Lightwave Technology*, vol. LT-5, no. 10, pp. 1339-1350, 1987.
- [3] J. Lee and D. M. Kim, "Analytic Time Domain Characterization of p-i-n Photodiodes: Effect of Drift, Diffusion, Recombination and Absorption," *Journal of Applied Physics*, vol. 71, no. 6, pp. 2950-2958, 1992.
- [4] J. B. Radunović and D. M. Gvozdić, "Nonstationary and Nonlinear Response of a p-i-n Photodiode Made of a Two-Valley Semiconductor," *IEEE Transactions on Electron Devices*, vol. 40, no. 7, pp. 1238-1244, 1993.
- [5] M. Dentan and B. de Cremoux, "Numerical Simulation of the Nonlinear Response of a p-i-n Photodiode Under High Illumination," *Journal of Lightwave Technology*, vol. 8, no. 8, pp. 1137-1144, 1990.
- [6] P. S. Matavulj, D. M. Gvozdić, J. B. Radunović, and J. M. Elazar, "Nonlinear Pulse Response of P-I-N Photodiode Caused by the Change of the Bias Voltage," *International Journal of Infrared and Millimeter Waves*, vol. 17, no. 9, pp. 1519-1528, 1996.
- [7] R. R. Hayes and D. L. Persechini, "Nonlinearity of p-i-n Photodetectors," *IEEE Photonics Technology Letters*, vol. 5, no. 1, pp. 70-72, 1993.
- [8] C. K. Sun, P. K. L. Yu, C.-T. Chang, and D. J. Albares, "Simulation and Interpretation of Fast Rise Time Light-Activated p-i-n Diode Switches," *IEEE Transactions on Electron Devices*, vol. 39, no. 10, pp. 2240-2247, 1992.